Urol Res (2012) 40:305–316
DOI 10.1007/s00240-011-0425-3

ORIGINAL PAPER

Distension of the renal pelvis in kidney stone patients: sensory and biomechanical responses

Katja Venborg Pedersen · Donghua Liao · Susanne Sloth Osther · Asbjørn Mohr Drewes · Hans Gregersen · Palle Jörn Sloth Osther

Received: 19 January 2011 / Accepted: 24 August 2011 / Published online: 10 September 2011

Abstract The pathogenesis of symptoms in urolithiasis is poorly understood. Traditionally increased endoluminal pressure is considered the main mechanism causing pain in the upper urinary tract but clinical data are sparse. The aim of the present study was to develop a new model related to mechanosensation in order to describe the geometric and mechanical properties of the renal pelvis in patients with kidney stone disease. Pressure measurement in the renal pelvis was done during CT-pyelography in 15 patients who underwent percutaneus nephrolithotomy. The sensory intensity was recorded at the thresholds for first sensation and for pain. 3D deformation and strain were calculated in five patients. The deformation of pelvis during distension was not uniform due to the complex geometry. The pelvis deformed to 113 ± 6% and 115 ± 11% in the longitudinal and circumferential directions, respectively. Endoluminal pressure in the renal pelvis corresponded positively to the sensory ratings but the referred pain area was diffuse located and varied in size. The present study provides a method for describing the mechanosensory properties and 3D deformation of the complex renal pelvis geometry. Although there was a relation between pressure and pain score, the non-homogenous spatial strain distribution suggests that the 3D biomechanical properties of the renal pelvis are not reflected by simple estimates of tension based on pressure and volume.

Keywords Pressure · Strain · Pain · Renal pelvis · Geometric model · Kidney stone

K. V. Pedersen · S. S. Osther · P. J. S. Osther (✉)
Urological Research Center, Department of Urology, Fredericia Hospital, Part of Hospital Littlebelt, University of Southern Denmark, Dronningensgade 97, 7000 Fredericia, Denmark
e-mail: pjo@urc.nu

D. Liao · A. M. Drewes · H. Gregersen
Mech-Sense, Department of Gastroenterology, Aalborg Hospital, Aarhus University Hospital, Aalborg, Denmark

H. Gregersen
Sino-Danish Centre for Education and Research, Aarhus, Denmark

H. Gregersen
Sino-Danish Centre for Education and Research, Bejiing, China

Introduction

The pathogenesis behind symptoms in urolithiasis is poorly understood and frequently there is a mismatch between disease severity and symptoms [1]. Traditionally endoluminal pressure is considered the main mechanism causing pain in the upper urinary tract but clinical data are sparse. Distension-induced deformation of the renal pelvis, for example as occurring in obstructive urolithiasis, activates mechanosensitive afferents in the pelvic wall [2]. Proper evaluation of structural and biomechanical properties of the renal pelvis may therefore contribute to the understanding of symptoms in urolithiasis and structural diseases such as hydronephrosis. Mechanosensitive receptors in the wall are the key link between mechanical stimuli and the resulting sensation. Gastrointestinal studies have indicated that mechanoreceptors are not directly sensitive to intraluminal volume or pressure as traditional pressure-volume measurements are biased by complex geometry [3]. Instead, the degree of tissue deformation (strain) and mechanical forces (stress) in circumferential direction seem to determine activation of the receptors [3]. Hence, methods for

describing the three-dimensional (3D) geometry and mechanical properties of complex visceral organs such as the gastrointestinal and the cardiovascular system based on cross-sectional imaging have been developed [4–8]. The objective of this study was to develop a method to describe the mechanosensory properties of the renal pelvis in patients with kidney stone disease, in other words this study can be considered as an experimental human model of visceral pain mechanisms made possible by the specific postoperative setup of percutaneous nephrolithotomy (PNL).

Materials and methods

Study subjects

Fifteen non-infection kidney stone patients (11 men, 4 women, mean age 54; range 32–79 years) were included. All patients underwent percutaneous nephrolithotomy (PNL) (lower pole puncture) before pressure measurement was performed during CT-pyelography. No major bleeding at the operation was observed and none of the patients was stented or had nephrostomy-catheter prior to surgery. Kidney stone characteristics are described in Table 1.

Study protocol

A standardized anaesthetic technique was used in all cases during PNL. The patient were premedicated with 1 g paracatamol and 75 mg diclofenac orally one hour before general anaesthesia, which was induced with infusions of propofol 10 ml/kg/h and remifentanil 60 μg/kg/h. Doses were halved after intubation. Anaesthesia was maintained with ramifentanyl infusion and sevofluran inhalation. Rocuronium was given for muscle relaxation. After completion of surgery, neuromuscular blockade was reversed with neostigmin. Every patient received 4 mg fortecontin at the beginning of the anaesthesia and 4 mg ondansetron at the end of the anaesthesia for antiemetic prophylaxis. At the end of the anaesthesia 0.1 mg/kg oxycodone or morphine was given intravenously and the surgeon injected 20 ml macaine 2.5 mg/ml into the incisional area. At the operation a Ch 24 nephrostomy-catheter was placed in the renal pelvis together with a 7 Fr selectip® catheter. Pain medication after surgery was individualized according to the patients pain VAS score. If needed the patients got opioids otherwise they were treated with paracetamol or Non-steroidal anti-inflammatory drugs on demand.

On the second day after PNL, a non-contrast CT-scan was done in all the patients. When correct placement of the selectip® catheter had been confirmed and perirenal hematoma was excluded, pelvis pressure measurement was initiated using the selectip® catheter connected to a transducer placed at kidney level and connected to a monitor (CardioMed CM-4008; Medistim, Oslo, Norway). When baseline pressure was reached contrast media (11% visipaque/NaCl) was injected into the nephrostomy-catheter with a flow rate of 1 ml/s using a motor pump (Medrad®). Sensory intensity during contrast injection was registered using a modified visual analogue scale (VAS) for both non-painful and painful sensations. The scale has been validated previously [4]. Before the study the patients were carefully instructed how to use the scale.

A CT-scan was recorded at VAS = 1 (sensory threshold) and VAS = 5 (pain threshold). Contrast injection was stopped temporarily at the sensory threshold and the patients were rotated from supine to prone position and back again to distribute the contrast medium in the renal pelvis before the first CT-scan. When baseline pressure was obtained, contrast medium was injected again to achieve the pain threshold and another scan was done. To reduce respiratory induced motion and associated artefacts the images were obtained during a single sustained breath hold.

The patients were asked to report the area of pain during distension caused by the contrast injection. Immediately after the scan, the patient marked the referred pain area at the pain threshold and it was drawn on a transparent paper. The area was digitised (ACECAD D 900+ Digitizer, Taiwan) and the size calculated electronically (Sigma-Scan, Jandel Scientific, Canada).

The study was monitored by the local Good Clinical Practice (GCP)-unit and approved by the Regional Ethics Committee. Oral and written informed consent was obtained from all patients and ICH-GCP guidelines were followed.

Image acquirement and 3D model reconstruction

Multi-Slice CT (Somatom Sensation 4, Siemens Healthcare, Erlangen, Germany) data were used to create 3D reconstructions of the kidney pelvis. The slice thickness was 2.5 mm with a helical pitch of 2. After the raw spiral CT data set were obtained, individual cross-sectional image slices were generated at 3 mm slices and 1 mm increment along the kidney pelvis and ureter in axial and coronal planes followed by 3D reconstructions. CT-scans from the five patients with high image quality were selected for model reconstruction.

Image processing

An edge detection program prior to computing the surface geometry defined the inner contours of the renal pelvis. It was computed semi-automatically for each orthogonal cross-sectional image by customized software based on gray tone thresholds (Fig. 1a, Interactive Data Language

Table 1 Clinical data for the patients

Patient No.	Stone size	Stone location	Duration of symptomatic stone disease	Pain	Referred pain area
1	20 mm	Lower calyx, left kidney	2 years	No pain for the last three months, before that periodic pain	3.57 cm^2
2	Many stones. The largest measured 13 mm	Lower calyx, left kidney	8 years	None	4.77 cm^2
3	Many stones. The two largest measured 15 and 12 mm	Lower calyx, left kidney	15 years	Once every year	8.74 cm^2
4	16 × 24 mm	Pelvis, right kidney	8 years	Almost every day for one year	16.95 cm^2
5	18 mm	Pelvis, left kidney	4 years	Once a week for the last 3 months	26.62 cm^2
6	Two stones, each measured 9 mm	Middle and lower calyx, right kidney	Periodic for 18 years	Almost every day for six months	48.21 cm^2
7	Six stones. The largest measured 20 mm	Pelvis, middle and lower calyx, left kidney	Years	Many pain colics	93.92 cm^2
8	20 mm	Pelvis, left kidney	2 years	Almost every day for 3 months	105.59 cm^2
9	8 mm	Pelvis, right kidney	6 months	Two or three times a week	225.77 cm^2
10	Many stones. The largest measured 17 mm	Lower calyx and pelvis, right kidney	6 months	No pain for the last two months, before that periodic pain	Did not reach pain threshold during distension
11	16 mm	Lower calyx, right kidney	9 months	None	Did not reach pain threshold during distension
12	Two stones at 15 and 7 mm	Pelvis and middle calyx, left kidney	5 months	Periodic pain	Did not reach pain threshold during distension
13	Two stones at 16 and 4 mm	Pelvis and lower calyx, right kidney	5–6 pain attacks during 40 years	5-6 pain attacks the last 40 years, no pain the last years	Did not reach pain threshold during distension
14	Two stones at 16 and 12 mm	Pelvis, left kidney	6 months	One pain attack. No pain the last month	Did not reach pain threshold during distension
15	Two stones at 14 and 10 mm	Middle and lower calyx, right kidney	2 years	None	Did not reach pain threshold during distension

6.0, Research Systems Inc., Boulder, CO, USA) and then adjusted if needed by two experienced radiologists. The transverse images were used to guide this adjustment.

Model reconstruction and surface smoothing

With the detected contours in each cross-sectional image (Fig. 1b), the 3D surfaces were subsequently extracted interactively using a custom Matlab subroutine (R14, The Mathworks Inc, USA).

Irregularities of reconstructed surfaces due to motion artefacts were reduced using the modified non-shrinking Gaussian smoothing method (Fig. 1c). The smoothed mesh was compared with the solid model and a good correlation was obtained.

Calculation of geometric characteristics

The approximate surface area and the volume of the pelvis at VAS = 1 and VAS = 5 were calculated as:

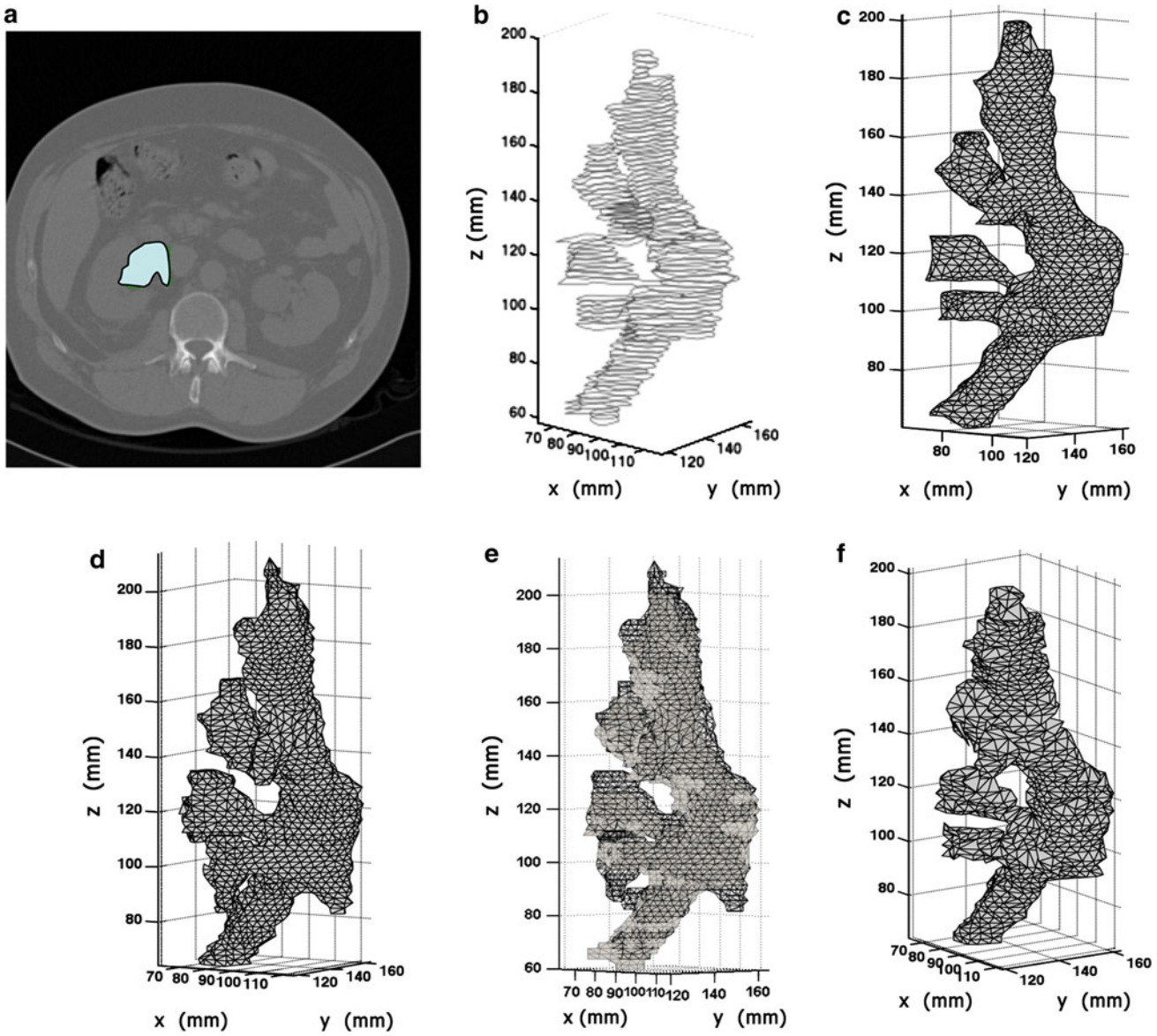

Fig. 1 An example illustrating the CT image processing and models matching. **a** One cross-sectional image with the boundary of the pelvis highlighted; **b** 3D contour generation on the basis of the segmented images; **c** 3D smoothed model on VAS = 1 with 1,856 vertexes (the total points of the models); **d** 3D reconstructed model on VAS = 5 with 2,158 surface points; **e** 3D models on VAS = 1 and VAS = 5 with the same central point on the first slices (Gray model VAS = 1, Black model, VAS = 5). It is evident that the large part of the gray model is inside the black model indicating the enlargement of VAS = 5; **f** the matched 3D model at VAS = 5 with the same amount of the surface points in model of VAS = 1

$$\text{surface area} = \sum_{i=1}^{n-1} 0.5(\text{arc}_i + \text{arc}_{i+1})h \quad (1)$$

$$\text{volume} = \sum_{i=1}^{n-1} 0.5(\text{area}_i + \text{area}_{i+1})h \quad (2)$$

where arc_i and area_i are the arc length and cross-sectional area at a given cross section i, h is the height between cross sections i and $i + 1$ and n is the total number of slices.

Displacement estimation

For deformation analysis, it is necessary to obtain the coordinates of every surface point at minimum two different deformation levels (in this study at VAS = 1 and VAS = 5). The original displacements on the surfaces of the renal pelvis after distension were obtained using the shape-tracking algorithm [9–11]. The method track points on successive surfaces using a shape similarity metric

which aims at minimizing the difference in principal curvatures. [1] It was validated previously using implanted markers [9].

The reconstructed 3D pelvis models at VAS = 1 and VAS = 5 from one patient were used as an example for describing the displacement estimation. The purpose for the displacement estimation was to find all points on surface s1 (Fig. 1c, surface at VAS = 1) and their symmetric nearest neighbour point on surface s2 (Fig. 1d, surface at VAS = 5). Before the displacement estimation, the models from two VAS levels were first adjusted to have the same central point on the first slice for eliminating the big movement during two distensions (Fig. 1e). The surface s2 was thus rebuilt as surface s3 based on the points matched to surface s1 (Fig. 1f). On the matched 3D surface s3, point p_1 on a surface s1 with VAS = 1 has a corresponding point p_2 on surface s3 at VAS = 5. The algorithm of the symmetric nearest neighbour point and the shape-tracking algorithm were described by Papademetris [10].

The displacement estimate vector u for each point p_1 between surface s1 and surface s3, is given by

$$u = p_2 - p_1, \tag{3}$$

Deformation and strain

The deformation of the surfaces between VAS = 1 and VAS = 5 are described by strain (a deformation ratio between the deformed and original geometry) distribution on the basis of the displace vector calculated in Eq. 3. The strains in the plane of the pelvis surface were computed based on the membrane assumption of the renal pelvis surface on each triangle faces on the surface model. The longitudinal and circumferential deformations were described by strain. Details on strain calculation are described in Appendix.

Using the above-described mathematical/geometric methods, this model enables us to obtain direct measurements of tissue strain in contrary to the indirect data obtained by just measuring pressure and volume.

Statistical analysis

Data are expressed as mean ± SE. Paired student t-test was used to detect differences between data on VAS = 1 and VAS = 5. All analyses were done using the software package Sigma Stat 2.0 (SPSS Inc. Chicago, USA).

[1] The curvature is a parameter of the geometrical property. The curvature of a curve is by definition the reciprocal of the radius of the osculating circle. The curvature is taken to be positive if the curve turns in the same direction as the surface's chosen normal, and otherwise negative. The smaller curvature the flatter is the surface.

Results

Pressure and sensory assessments during distensions

The average baseline pressure was 13 mmHg (range 6–20 mmHg). The renal pelvis pressure increased during contrast injection in all patients and they all felt a vague perception of mild sensation corresponding to VAS = 1. After this the patient was removed from the tranducers zero level for a short period of time and due to the rotation procedure there was a false pressure increase, after which baseline pressure was obtained again (Fig. 2). A distension corresponding to the pain threshold (VAS = 5) was only achieved in nine patients. In the remaining patients, this could not be achieved due to fast passage of the contrast to the bladder. The average pressure at VAS = 1 and VAS = 5 was 27 mmHg (range 13–50 mmHg) and 34 mmHg (range 20–53 mmHg), respectively (Fig. 2). The pressure increase from VAS 1 to VAS 5 was statistically significant ($P < 0.001$). When contrast injection was stopped, the pressure normalized. Because of technical problems, pressure recordings from two patients were excluded.

The referred pain area to distension was measured in the nine patients, who reached the pain threshold. The area varied in location and size; in six patients, it was located under the 12th rib, in one patient in the mid axillary line and in two patients on the lower abdominal wall (Fig. 3). No patient complained of testicular/groin pain. A major variation was found in the size of the referred pain areas; from 3.6 to 225.8 cm^2. There was no obvious relationship between the number of stone colics the patients had experienced prior to surgery and the size of referred pain area (Table 1).

Geometric description of the model before and after distensions

The pelvis deformed both longitudinally and circumferentially from VAS = 1 to VAS = 5. The surface area and volume increased 16.8 and 35.8% from VAS = 1 to VAS = 5, respectively (Table 2). Using calculation of geometric characteristics, it was obvious that the distension-induced extension of the pelvis was not uniform due to the complexity of the initial geometry and the large deformation. The principal curvature distributions indicated the complex geometry of the pelvis as well as the orientation of the principal curvatures, i.e., the first principal curvatures were mostly located in

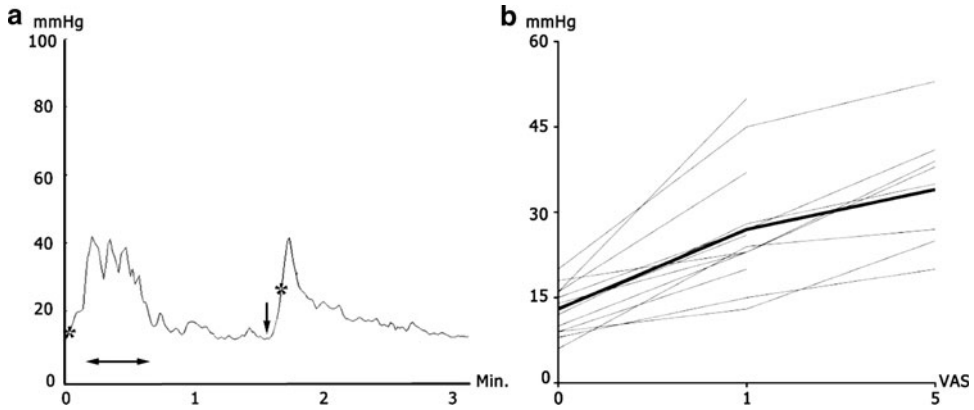

Fig. 2 **a** Typical pressure recordings from a patient during CT-pyelography. The *far left asterisk* denotes the sensory threshold and the *far right asterisk* denotes the pain threshold. The *large horizontal arrow* shows the pressure rise due to rotation and the *small vertical arrow* denotes injection of contrast media. **b**: Pressure as a function of the sensation score registered using a modified visual analogue scale (VAS) with one being the sensation threshold and five the pain threshold. Each graph represents one patient and the bold graph represents the mean score

the circumferential direction and the second principal curvatures mostly in the longitudinal direction[2] (Fig. 4a, b).

3D displacement distribution after distension

The displacement distribution indicated the non-homogeneous movement of the pelvis after distension and the orientation of the displacement showed the extension of the model (Fig. 5a). The distension-induced displacement was attributed to both the pelvis deformation and rigid movements of the pelvis. The rigid movement had no contribution to the pelvis deformation. Hence, defining a parameter; such as strain seems important to describe the pure deformation of the pelvis during distension.

3D strain distribution

The average strain increased when the pressure difference between two VAS levels increased. A typical strain distribution showed that deformation mostly occurred in the circumferential direction indicating the enlargement of the pelvis (Fig. 5b, c). The histogram graph of the strain distribution showed different distributions between the circumferential strain and the longitudinal strain (Fig. 5d, e). The summarized strain distribution showed that deformation happened in both circumferential and longitudinal directions and there was no difference between the strains in these two orientations (Table 3).

Discussion

The present study describes to our knowledge for the first time the 3D geometry and the mechanosensory properties of the human renal pelvis. The study represent an experimental human model of visceral pain that was made possible due to the specific postoperative setting after a PNL, in which a catheter is placed in the renal pelvis making experimental distension and pressure measurement as well as advanced imaging possible. The main findings were that (1) the distension-induced extension of the pelvis was not uniform due to the complexity of the geometry; (2) endoluminal pressure in the renal pelvis corresponded positively to the pain VAS score and (3) the referred pain area was diffusely located and varied in size.

Advantages and limitations of the present study

The present method based on cross-sectional imaging shows how the 3D geometry of the complex renal pelvis surface may be characterized. We refrained from calculation of the tension using simple mechanical laws as Laplace's law since it only works for simple geometry with positive surface curvatures. The current method allows us to measure the combined (circumferential and longitudinal) strain and curvatures. These parameters provide a more comprehensive description of potential factors stimulating mechanosensitive afferents. However,

[2] At each point P of a differentiable surface in 3D Euclidean space, a normal plane at P is one that contains the normal, and will therefore also contain a unique direction tangent to the surface and cut the surface in a plane curve. This curve will in general have different curvatures for different normal planes at P. The principal curvatures and second principal curvature at p are the maximum and minimum values of this curvature.

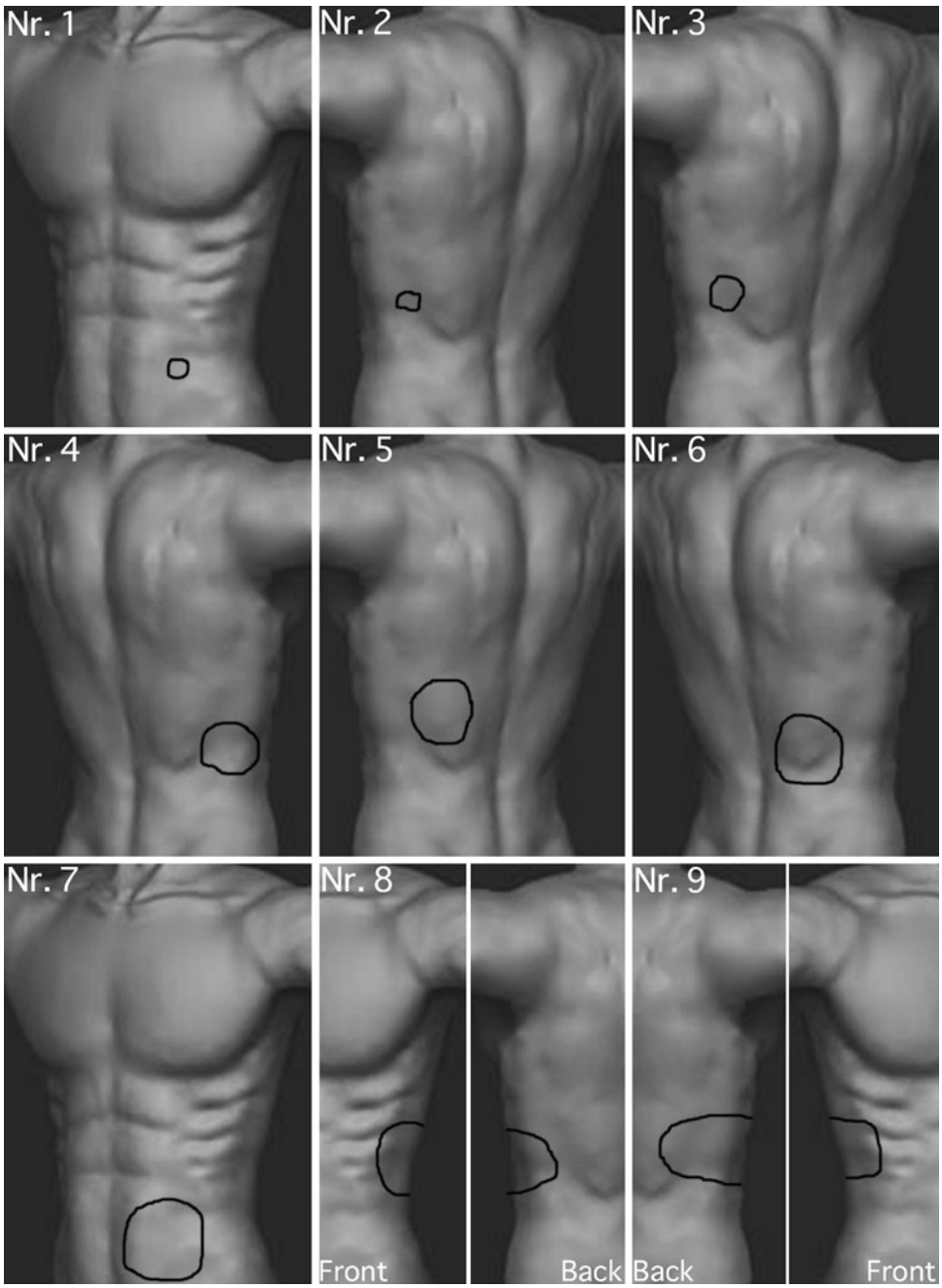

Fig. 3 Approximately size and location of the referred pain area for the nine patients who experienced pain during distension

Table 2 Basic geometric parameters of the renal pelvis at sensory threshold and pain threshold

	Surface area (cm^2)*	Volume (ml)*	Maximum Length (cm)[#]	Maximum circumference (cm)[§]
Sensory threshold	160.5 ± 14.9	53.8 ± 7.68	16.3 ± 1.03	18.8 ± 0.78
Pain threshold	187.5 ± 14.5	72.0 ± 8.16	16.7 ± 1.23	19.1 ± 1.33
Ratio (pain threshold/sensory threshold)	1.18 ± 0.13	1.41 ± 0.37	1.02 ± 0.03	1.02 ± 0.12

* $P < 0.05$ Comparing data between sensory threshold and pain threshold

[#] Maximally obtained length of pelvis during distension

[§] Maximally obtained circumference of pelvis during distension

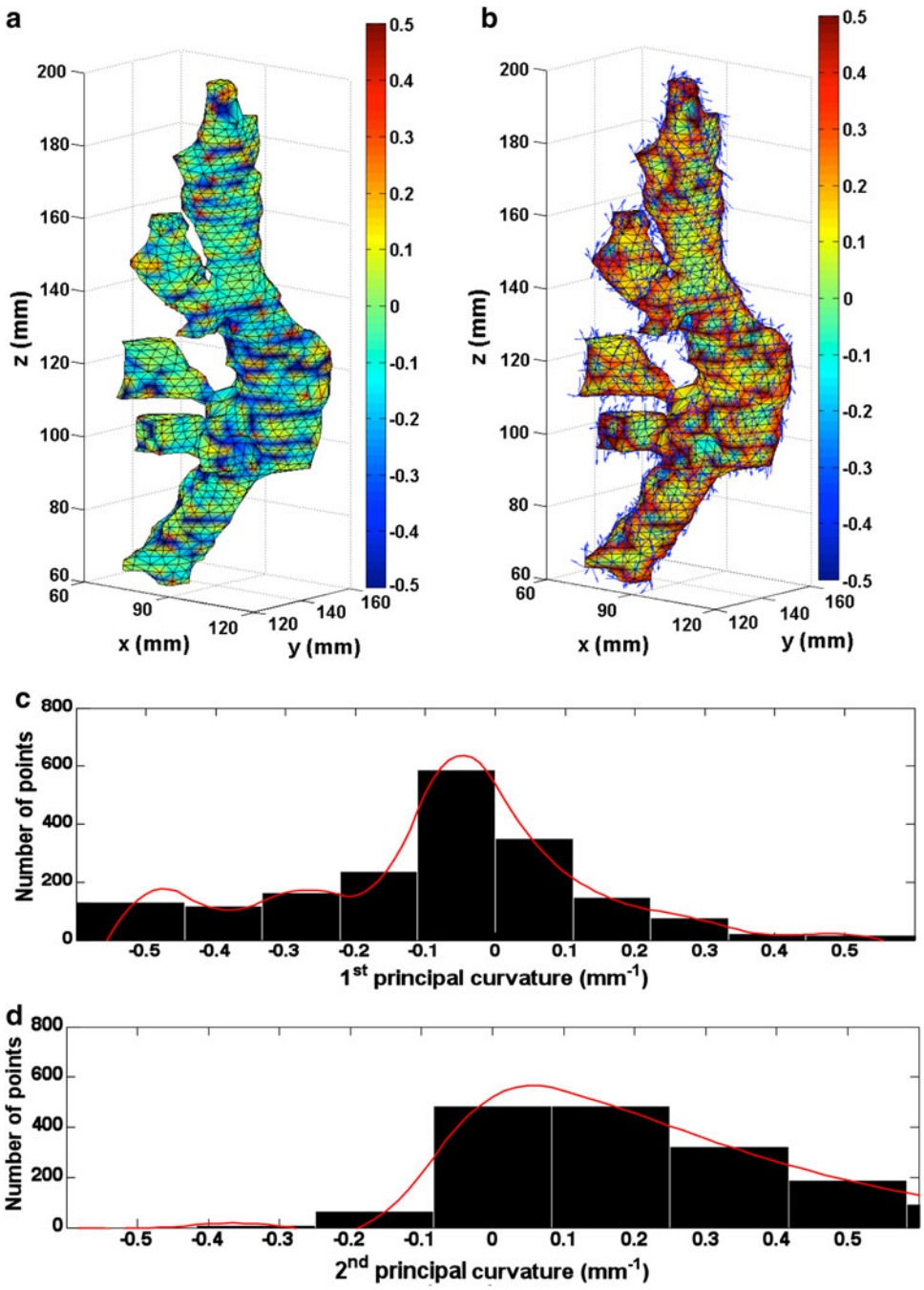

Fig. 4 An example of the principal curvature distributions. **a** The first principal curvature, mainly in the circumferential direction (the smaller curvature, the more flat the surface). **b** The second principal curvature distribution, mainly in the longitudinal direction (*blue arrows*). **c** The histogram of the first principal curvature distribution and **d** The histogram of the second principal curvature distribution. The non-uniform distributions of the principal curvatures were due to the complex geometry of the pelvis

the data represent the first approach to make such a model and may be considered a pilot study to guide future developments.

Using CT, the correct placement of catheters and contrast media could be visualized and controlled. The limitations of the present technique was the time delay from the patient reported VAS = 1 or VAS = 5 to the CT-scan was done due to rotation of the patient. This was, however, necessary to define the exact geometry. The degree of pelvic dilatation on CT pictures may therefore have been underestimated due to volume evacuation or viscoelastic properties (stress-relaxation).

Mechanical and mechanosensory properties of the renal pelvis

This study gave detailed information about renal pelvis configuration; such as principal curvatures and strain distribution, which make it possible to determine regional geometry and strain. Animal studies have identified two

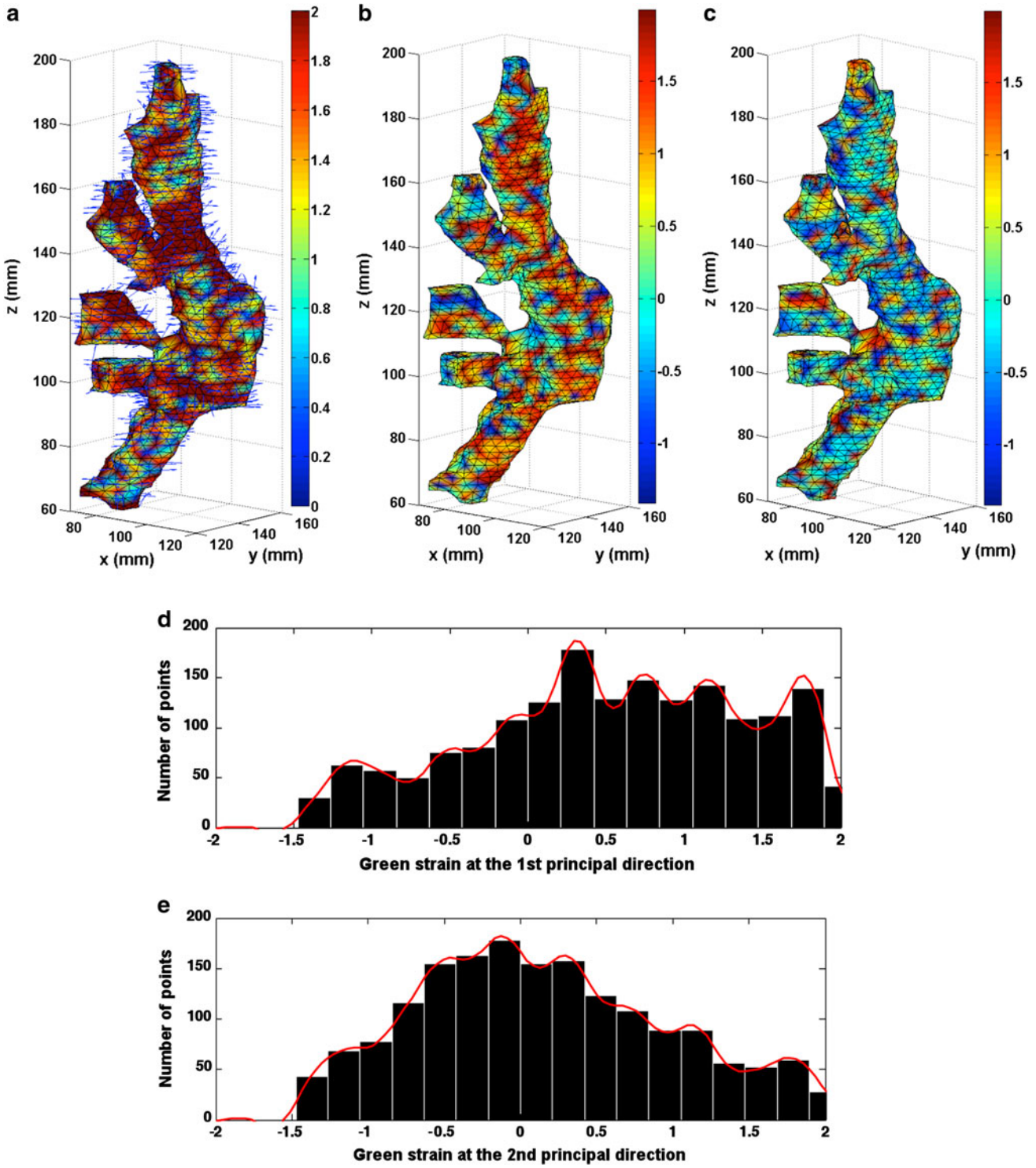

Fig. 5 Distension-induced displacement and strain distributions on a typical model. **a** Distension-induced displacement distribution with the *blue arrows* indicating the direction of the displacement. **b** 3D strain distribution on the first principal curvature direction (mainly in the circumferential direction). **c** 3D strain distribution on the second principal curvature direction (mainly in the longitudinal direction). The *colour from blue to red* indicates the increase of the value. The mostly red colour in panel **b** indicated a bigger circumferential distension on this sample. **d**, **e** Histograms of the circumferential and longitudinal strain distribution showing a bigger circumferential strain tendency

Table 3 Circumferential and longitudinal strain distributions

	Average	Maximum	Minimum
Circumferential	0.15 ± 0.11	1.06 ± 0.35	−0.65 ± 0.27
Longitudinal	0.13 ± 0.06	1.05 ± 0.34	−0.66 ± 0.23

major types of sensory receptors in the renal pelvis, mechanoreceptors responding to pressure increase and chemoreceptors sensitive to urine ion composition and renal ischemia. These receptors are important for kidney function and probably sensation [2, 12]. However, mechanical deformation of nerve endings produced by stretch is believed to be the primary mechanism of mechanoreceptor activation rather than variation in endoluminal pressure [12]. The neurons respond in an intensity-dependent manner to stimuli [2, 12]. Hence, determination of strain locally is important for understanding the mechanical environment at receptor sites. The higher strain sites are expected to be more sensitive [13, 14]. The non-uniform deformation during renal pelvis distension demonstrated in this study may reflect the non-homogeneous stiffness distribution of the pelvis wall.

The physiological renal pelvis pressure in humans has been reported to be in the range 0–10 mmHg [15], and prior to ureterorenoscopy in the range of 12–14 mmHg [16, 17]. In the present study, the mean intraluminal baseline pressure was 13 mmHg (range 6–20 mmHg), which thus correlates well with data in the literature.

At the pain threshold, we found the mean pelvis pressure to be 34 mmHg (range 20–53 mmHg). This is in agreement with the only other human study reported in the literature, in which the pain threshold was found to be at a pelvis pressure of 33 mmHg (range 21–58 mmHg) [18].

No sensation occurred in the beginning of the pressure rise. After reaching the sensory threshold, the perception increased rapidly to the pain threshold. One explanation for this could be that sensation may be associated with activation of high threshold receptors. In the guinea pig ureter, two types of mechanoreceptors have been found. High threshold receptors that did not respond to peristalsis but to intense distensions (mean 25 mmHg)—believed to have nociceptive functions—and low threshold receptors (mean 8 mmHg) that responded to contractions of the ureter monitoring peristalsis [19].

In experimental studies, it have been shown that repeated painful stimulation (mimicking the sensitized state in disease) of the stomach, colon and bladder caused increased referred pain areas, probably due to central sensitization of the nervous system [20]. In the present study, we found no obvious relationship between the number of stone colics prior to surgery and the size of referred pain area. This may be due to the limited sample number.

In this study, we found that pelvis distension resulted in referred pain area located to the subcostal region, the midaxillary line and the lower abdominal wall. No patients complained of testicular/groin pain which must be an indirect expression of that referred pain area in this location is the result of ureteral involvement/distension.

Conclusion

Although there was a relation between pressure and pain score, the non-homogenous spatial strain distribution suggests that simple estimates of tension based on pressure and volume do not reflect the 3D biomechanical properties of the renal pelvis. 3D modelling may be used for understanding biomechanical properties and visceral perception in the renal pelvis. In the future, this may be useful for our understanding of conditions such as hydronephrosis and pain originating from the upper urinary tract.

Acknowledgments This study was supported by the Beckett Foundation and the Local Research Foundation of Fredericia and Kolding Hospitals. Thanks to Elena Steffensen, Department of Radiology, Aalborg Hospital, Aarhus University Hospital, Aalborg, Denmark, for helping with image segmentation. Thanks to Ole Graumann, Urological Research Center, Hospital Littlebelt, Fredericia, Denmark, for helping with figure creation.

Appendix

Strain calculation

The membrane strain in every triangle plane can be defined with the displacement of every point on the surface and the coordinates of each three points that define a triangle determine a plane. The coordinates of these points in that plane at VAS = 1 are denoted as x_i and y_i ($i = 1, 2, 3$, are three points of the plane). The displacement in the local system of the points at VAS = 1 to their position at VAS = 5 are denoted as u_i, v_i and w_i (u, v and w are, respectively, the displacement in x, y, and z directions, Fig. 6).

The displacements are assumed to be in a displacement field that is a linear function of position in the plane of the triangle. For example

$$u_i = a_1 + a_2 x_i + a_3 y_i \, (i = 1, 2, 3) \tag{A1}$$

This equation with known displacement and the position of three markers substituted for u_i, x_i and y_i provides a set of three equations for the three coefficients, a_1, a_2 and a_3.

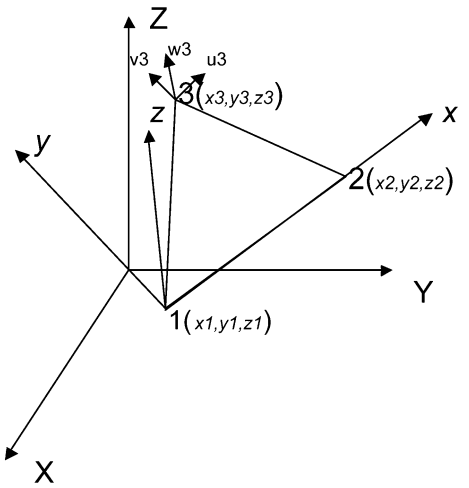

Fig. 6 Schematic diagram of the global coordinate system XYZ and the local coordinate system xyz on one triangle face with nodes 1, 2, and 3 at VAS = 1. The displacement at the local coordinate system on the node 3 (u3, v3 and w3) is illustrated as an example. All strains were calculated based on the local coordinate system. For details about the transformation between the global coordinate system and the local coordinate system, see [21]

Similarly, the data provide the information required to determine the coefficients in the following equations

$$\begin{aligned} v_i &= a_4 + a_5 x_i + a_6 y_i \\ w_i &= a_7 + a_8 x_i + a_9 y_i \end{aligned} \tag{A2}$$

where $a_4 \cdots a_9$ are coefficients that could be defined with known displacement (v_i and w_i) between surface of VAS = 1 and VAS = 5 and coordinates (x_i and y_i) on surface of VAS = 1

The components of the Green strain in the plane are defined by the following equations

$$\begin{aligned} E_{xx} &= \frac{\partial u}{\partial x} + 0.5\left[\left(\frac{\partial u}{\partial x}\right)^2 + \left(\frac{\partial v}{\partial x}\right)^2 + \left(\frac{\partial w}{\partial x}\right)^2\right] \\ E_{yy} &= \frac{\partial v}{\partial y} + 0.5\left[\left(\frac{\partial u}{\partial y}\right)^2 + \left(\frac{\partial v}{\partial y}\right)^2 + \left(\frac{\partial w}{\partial y}\right)^2\right] \\ E_{xy} &= \frac{\partial u}{\partial y} + \frac{\partial v}{\partial x} + 0.5\left(\frac{\partial u}{\partial x}\frac{\partial u}{\partial y} + \frac{\partial v}{\partial x}\frac{\partial v}{\partial y} + \frac{\partial w}{\partial x}\frac{\partial w}{\partial y}\right) \end{aligned} \tag{A3}$$

with the known coefficients $a_1 \cdots a_9$ and substituting Eqs. A1 and A2 into A3, the strain on the triangle plane can thus be obtained.

The principal strain and the corresponding principal orientation are calculated from:

$$\begin{bmatrix} E_{11} & 0 \\ 0 & E_{22} \end{bmatrix} = \begin{bmatrix} l_1 & l_2 \\ m_1 & m_2 \end{bmatrix} \begin{bmatrix} E_{xx} & E_{xy} \\ E_{xy} & E_{yy} \end{bmatrix} \begin{bmatrix} l_1 & l_2 \\ m_1 & m_2 \end{bmatrix}^T \tag{A4}$$

where E_{11}, E_{22} are principal strains and $\{l_1, m_1\}^{\mathrm{T}}$ and $\{l_2, m_2\}^{\mathrm{T}}$ are corresponding principal directions in the local coordinate system. There is no shear strain in the principal directions. T means transpose of the matrix or vectors.

The equivalent strain is defined as:

$$e = \sqrt{\frac{2}{9}\left(\left(E_{xx} - E_{yy}\right)^2 + E_{xx}^2 + E_{yy}^2 + 6E_{xy}^2\right)} \tag{A5}$$

References

1. Pedersen KV, Drewes AM, Frimodt-Møller FC et al (2010) Visceral pain originating from the upper urinary tract. Urol Res 38:345–355
2. Ammons WS (1992) Renal afferent inputs to ascending spinal pathways. Am J Physiol 262:165–176
3. Gregersen H (2003) Gastrointestinal smooth muscle mechanical behaviour and neural circuits, Chap 5. In: Biomechanics of the gastrointestinal tract, Springer, Berlin, pp 137–180
4. Drewes AM, Gregersen H, Arendt-Nielsen L (2003) Experimental pain in gastroenterology. A reappraisal of human studies. Scand J Gastroenterol 38:1115
5. Fillinger MF, Raghaven ML, Marra SP et al (2002) In vivo analysis of mechanical wall stress and abdominal aortic aneurysm rupture risk. J Vasc Surg 36:589–597
6. O'Dell WG, McCulloch AD (2000) Imaging three-dimensional cardiac function. Annu Rev Biomed Eng 2:431–456
7. Liao D, Gregersen H, Hausken T et al (2004) Analysis of surface geometry of the human stomach using real-time 3-D ultrasonography in vivo. Neurogastroenterol Motil 16:315–324
8. Liao D, Duch BU, Stodkilde-Jorgensen H et al (2004) Tension and stress alculations in a 3-D Fourier model of gall bladder geometry obtained from MR images. Ann Biomed Eng 32:744–755
9. Shi P, Sinusas AJ, Constable RT et al (2000) Point-tracked quantitative analysis of left ventricular surface motion from 3-D image sequences. IEEE Trans Med Imaging 19:36–50
10. Papademetris X (2000) Estimation of 3D Left ventricular deformation from medical images using biomechanical models, Ph.D. Dissertation, Yale University, New Haven, CT. http://noodle.med.yale.edu/thesis, accessed May 2000
11. Papademetris X, Sinusas AJ, Dione DP et al (2001) Estimation of 3D left ventricular deformation from echocardiography. Med Image Anal 5:17–28
12. Kopp UC, Smith LA, Pence L (1994) Na^+–K^+ ATPase inhibition sensitizes renal mechanoreceptors activated by increases in renal pelvic pressure. Am J Physiol Regul Integr Comp Physiol 267:1109–1117
13. Page AJ, Martin CM, Blackshaw LA (2002) Vagal mechanoreceptors and chemoreceptors in mouse stomach and esophagus. J Neurophysiol 87:2095–2103
14. Phillips RJ, Powley TL (2000) Tension and stretch receptors in gastrointestinal smooth muscle: re-evalusting vagal mechanoreceptor eletrophysiology. Brain Res Rev 34:1–26
15. Djurhuus J C (1980) Aspects of renal pelvic function, Thesis; University of Copenhagen
16. Jung H, Nørby B, Frimodt-Møller PC et al (2008) Endoluminal isoproterenol irrigation decrease renal pelvic pressure during flexible ureterorenoscopy: a clinical randomized, controlled study. Eur J Urol 54:1404–1413
17. Auge BK, Pietrow PK, Lallas CD et al (2004) Ureteral access sheath provides protection against elevated renal pressures during routine flexible ureteroscopic stone manipulation. J Endourol 18:33–36

18. Risholm L (1954) Studies on renal colic and its treatment by posterior splanchnic block. Acta chir Scand suppl 184:1–64
19. Cervero F, Sann H (1989) Mechanically evoked responses of afferent fibres innervating the guinea-pigs ureter: an in vitro study. J Physiol 412:245–266
20. Arendt-Nielsen L, Laursen RJ, Drewes AM (2000) Referred pain as an indicator of neural plasticity. Prog Brain Res 129:343–356
21. Fung YC (1977) Analysis of strain, foundations of solid mechanics, Chap 4. Prentice-Hall international INC, Englewood Cliffs, pp 89–108